JOURNAL OF Materials CHEMISTRY

Gas-sensitive resistor properties of the solid solution series $Ti_x(Sn_{1-y}Sb_y)_{1-x}O_2$ ($0<x<1$, $y=0$, 0.01, 0.05)

Vincent Dusastre and David E. Williams*

Department of Chemistry, University College London, 20 Gordon Street, London, UK WC1H OAJ. E-mail: d.e.williams@ucl.ac.uk

Received 22nd September 1998, Accepted 24th November 1998

The response to carbon monoxide, methane and water vapour of gas-sensitive resistors fabricated from solid solution compounds $Ti_x(Sn_{1-y}Sb_y)_{1-x}O_2$ where $0<x<1$ and $y=0$, 0.01, 0.05 has been studied. For the single phase materials the variation of both conductance and conductance activation energy with composition has been explained using either a surface trap limited conductance model for undoped materials or a Schottky barrier controlled conductance for Sb-doped materials. The effect of dopant density and surface composition on the gas response has been explained using a compensated semiconductor conduction model. The surface states controlling response to water vapour are not the same as those controlling response to the combustible gases. The adsorbed oxygen states responsible for gas sensitivity lie closer to the conduction band edge for TiO_2 than for SnO_2. The surface oxygen states and surface water states are closer in energy on TiO_2 than on SnO_2. The resistivity and gas sensitivity of spinodally decomposed materials could be interpreted in terms of the phase diagram which indicated no differences from the behaviour of the single-phase components.

Introduction

There is an extensive literature describing the investigation of variations in composition of tin dioxide-based gas-sensitive resistors, seeking improved sensitivity, selectivity and long term stability as sensors for hydrocarbon gases. Composites such as ZnO–SnO_2[1] and solid solutions such as SnO_2–TiO_2[2,3] are examples. TiO_2 and SnO_2 gas sensor materials have been widely used at elevated temperature for combustible and toxic gas detection: CO, hydrocarbons, alcohols and NO_x.[4] It has also been reported that the (Ti–Sn)O_2 system can be used at room temperature as a stable humidity sensor,[5,6] the effect being attributed to a conductivity increase induced by excess proton conduction in a physisorbed multilayer of water.

Tin and titanium dioxides show the same rutile structure and form a complete solid solution at 1430 °C which undergoes spinodal decomposition upon annealling at lower temperature.[7,8] Both oxides show n-type semiconductivity induced by oxygen-deficient defect structures, in which donor levels are formed by electrons trapped on cations associated with oxygen vacancies (formulae as written subsequently do not preclude the possibility of such oxygen deficiency). The electrical conductivity is enhanced by appropriate doping (Nb for TiO_2 and Sb for SnO_2). It has been observed that the complete ionisation of donor levels introduced by these dopants takes place at lower temperature in SnO_2 than in TiO_2, which explains why the electrical resistivity of Sb-doped SnO_2 is several orders of magnitude lower than that of Nb-doped TiO_2.[9]

SnO_2 and TiO_2 also exhibit rather different surface properties. On the surface of oxide catalysts and zeolites, Ti cations act as Lewis acid sites.[10] Lewis acidity strength is expected to depend on the ion charge, the degree of coordinative unsaturation and the availability of empty orbitals (*i.e.* the bandgap). Whereas removal of oxygens from SnO_2 leading to the formation of surface Sn^{2+} (with a pair of electrons occupying the Sn 5s orbitals) is expected to inhibit the acid–base interaction, strong Lewis acidity is expected with Ti^{4+} surface species.[11] Therefore, if there were some effect of the acid–base character of the oxide surface upon the processes which give rise to electrical conductivity changes, it could show up in the behaviour of the (Ti–Sn)O_2 solid solution. A previous description of SnO_2–TiO_2 thick film gas sensors showed a maximum in sensitivity to CH_4 with composition upon introducing 5% mol TiO_2.[2,3] These authors interpreted these effects as due to the inter-grain Schottky barrier height becoming higher upon doping with TiO_2.

The tetragonal TiO_2–SnO_2 solid solution system contains a subsolidus immiscibility gap[8] with a critical temperature, T_c, of around 1400 °C (varying according to different authors[7,8,12]), inside which phase separation is characterised by coherent spinodal decomposition corresponding to [001] modulations.[8,13,14] A study of decomposition rates outside the region of spinodal decomposition suggested that the ionic mobility of diffusing tin was much slower than that of titanium in the alloy system.[15] Furthermore, aliovalent dopants are expected to affect the kinetics of phase separation either by a nucleation and growth mechanism or by a cellular mechanism.[16] Doping with pentavalent species is expected to decrease the cation interstitial concentration and thereby decrease the rate of phase separation.[17,18] Doping with antimony(v) atoms has been shown to strongly suppress the phase separation both inside and outside the region of spinodal decomposition.[15] Therefore, this solid solution system also offers the opportunity to study the consequences, if any, of the new boundaries introduced by spinodal decomposition upon the electrical response to gas reaction on the surface.

In this paper we report a systematic study of the series of compounds $(Sn_{1-y}Sb_y)_{1-x}Ti_xO_2$ ($0\leqslant x\leqslant 1$, $y=0$, 0.01, 0.05). The response to humidity, carbon monoxide, methane and propane has been examined. The effects of preparation methods, composition, Sb-doping and changes in surface composition on electrical properties and gas sensing characteristics have been investigated. The results have been assessed against the simple model for composition dependence of gas-sensitivity developed by Williams and Moseley.[19] This model adequately described the behaviour of our materials.

Experimental

The series of compounds $Ti_x(Sn_{1-y}Sb_y)_{1-x}O_2$ ($0<x<1$, $y=$ 0, 0.01, 0.05) was prepared by milling in acetone for 24 hours stoichiometric amounts of SnO_2, TiO_2, and Sb_2O_5 (all Fluka, 99% pure). The acetone was then evaporated and the resultant powders were subjected to an annealing treatment at 1400 °C

for 2 hours and allowed to cool quickly in order to obtain single-phase solid solutions, as confirmed by XRD. The samples were subsequently fired in a furnace at 1000 °C for 12 hours. The compounds were ground, pressed to 1 ton into about 1.5 mm thick pellets (13 mm in diameter) and sintered at 900 °C for 12 hours. A new series of materials $Ti_xSn_{1-x}O_2$ and $Ti_x(Sn_{0.95}Sb_{0.05})_{1-x}O_2$ ($x<0.3$) was prepared by mixing the powders in water with a high shear mixer (a 'homogeniser') using control of pH and a non-ionic surfactant to promote dispersion. The water was removed under reduced pressure in a rotary evaporator with the flask immersed in an ultrasonic bath, so that the dispersion and mixing of the powders was maintained throughout the evaporation. These powders were subsequently fired at 800, 1000, and 1200 °C to study the effect of the microstructure and spinodal decomposition on the sensitivity to different gases and are referred to in the following as 'homogenised'.

Electrical conductivity in a controlled gas atmosphere was measured[20] by clamping the pellets between gold electrodes using an alumina jig, mounted in a silica tube inside a tube furnace. Resistance measurements were simply two-terminal DC measurements made using a digital multimeter. This is not a method recommended for high-accuracy measurements but we have repeatedly shown it to be reliable and repeatable for comparisons of the type which we wish to make here. Polarisation effects at the electrodes show up as large apparent jumps in resistance when the multimeter changes range: such effects were absent. Results are reported as an apparent resistivity, taking account of the external dimensions of the pellets; the values would, of course, be dependent on the details of porosity and microstructure of the pellets.

X-Ray powder diffractometry (Siemens D5000, Cu-Kα radiation) demonstrated a phase pure rutile structure (solid solution) across the whole series for materials annealed at 1400 °C. X-Ray photoelectron spectroscopy (XPS) measurements were carried out using monochromated Al-Kα X-rays ($E=1486.6$ eV) with a 300 μm spot size. The spectra were acquired with a step size of 50 meV and with an analyser pass energy of 20 eV. Sample charging was controlled using a 3 eV electron flood gun. The binding energies were referenced to the adventitious hydrocarbon C 1s peak at 284.8 eV. Quantifications were performed using a Shirley background and sensitivity factors were obtained from Wagner.[21] The sample pressure was $<5\times10^{-10}$ mbar.

Results

Characterisation of the materials

XRD patterns confirmed that solid solution with rutile structure was achieved for the complete range, $0\leqslant x\leqslant 1$ for materials prepared by the ball-milling method. Fig. 1 shows the a and c parameters of $Ti(Sn–Sb)O_2$ solid solutions as a function of TiO_2 mole ratio, including the pure end components.

Both lattice parameter (a, c) values decreased with TiO_2 mole ratio following Vegard's law, due to the smaller ionic radius of Ti^{4+} (0.61 Å) *vs.* Sn^{4+} (0.69 Å). Furthermore, the decrease in the lattice parameters due to antimony substitution suggests that the Sb component of the solid solution must mostly comprise Sb^{5+}, which is small enough to contract the $(TiSn)O_2$ lattice, since its ionic radius is 0.60 Å compared to 0.76 Å for Sb^{3+}.

As expected, the comparison between two identical materials prepared by a different method showed (Fig. 2), firstly, the appearance of the spinodal decomposition for materials fired at lower temperature, and secondly that powders with a lower particle size (calculated with the Scherrer equation) could be prepared by using the homogenisation method (Table 1).

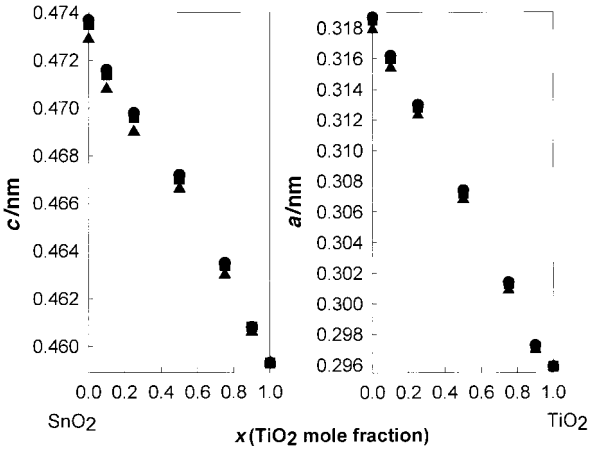

Fig. 1 Lattice parameter (a,c) as a function of composition x in $Ti_x(Sn_{1-y}Sb_yO_2)_{1-x}$ solid solution preparations; $y=0$ (●), 0.01 (■), 0.05 (▲).

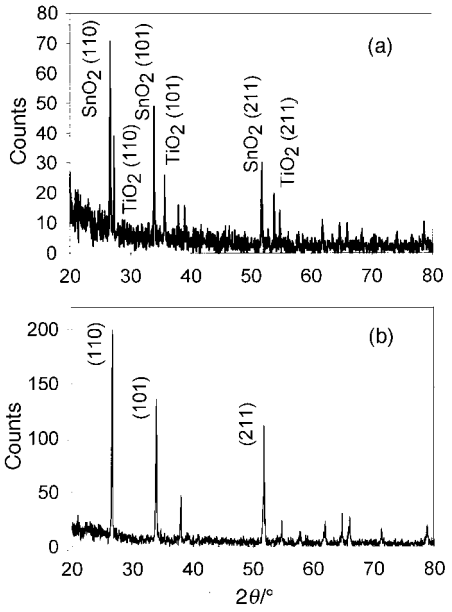

Fig. 2 X-Ray diffraction patterns of $Ti_{0.75}(Sn_{0.99}Sb_{0.01})_{0.75}O_2$ showing the appearance (a) of spinodal decomposition in material fired at 1000 °C for 20 h and the formation (b) of a solid solution for material fired at 1400 °C for 12 h.

There is the possibility also, that reaction between the two components was only partial at the lower firing temperatures.

As expected the particle size increased with increasing sintering temperature. The specific surface areas, obtained from BET isotherm data of Kr adsorption at −196 °C, slightly decreased from 1.7 to 1.0 $m^2\ g^{-1}$ for materials respectively sintered at 800 and 1200 °C. Doping with Sb had the effect of decreasing the particle size.

Sb surface analysis determined by XPS using the Sb $3d_{3/2}$ peak since the $3d_{5/2}$ peak overlapped with O 1s confirmed that Sb was surface enriched in the $Ti(SnSb)O_2$ series as can be seen on Fig. 3, the segregation being possibly driven by Sb^{3+} formation.[22] The oxygen : metal ratio increased steadily across the series. Table 2 shows electron binding energies for tin, titanium and antimony for the 1% Sb-doped materials. The Ti $2p_{3/2}$ binding energies for the mixed metal oxides were slightly higher than for TiO_2. No evidence of lower oxidation surface states for Ti was observed.

Table 1 Comparison of particle sizes for materials sintered at different temperatures and prepared by different methods

	Sintering temperature/°C			
	800	1000		1200
	$Ti_{0.1}Sn_{0.9}O_2$			
	Particle size/nm by XRD	$Ti_{0.1}Sn_{0.9}O_2$	$Ti_{0.1}(Sn_{0.95}Sb_{0.05})_{0.1}O_2$	$Ti_{0.1}Sn_{0.9}O_2$
Homogenisation	89	95	80	96
Ball-milling	108	114	102	117

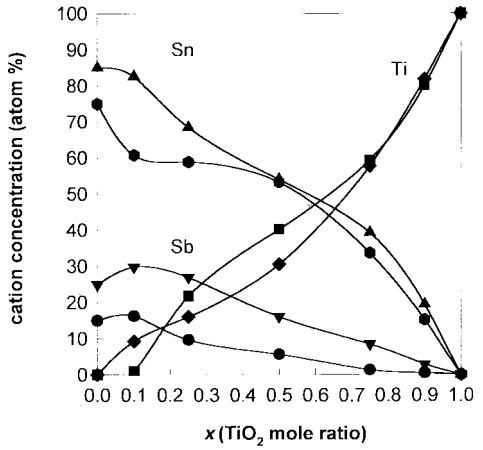

Fig. 3 Surface concentration of cations (atom%), expressed as a fraction of the total surface cation concentration, as a function of composition for solid-solution $Ti_x(Sn_{1-y}Sb_yO_2)_{1-x}$; (●) %Sb, $y=0.01$; (■) %Ti, $y=0.01$; (▲) %Sn, $y=0.01$; (▼) %Sb, $y=0.05$; (◆) %Ti, $y=0.05$; (⬢) %Sn, $y=0.05$.

Table 2 Electron binding energies E_b (eV) for $Ti_x(Sn_{0.99}Sb_{0.01})_{1-x}O_2$

Composition (x)	Ti $2p_{3/2}$	Sn $3d_{5/2}$	Sb $3d_{3/2}$
0.1	459.25	487.31	540.91
0.25	459.31	487.25	540.66
0.5	459.38	487.19	540.66
0.75	459.50	487.38	541.00
0.9	459.38	487.63	541.41
1	458.70	—	—

Electrical properties and gas-sensing characteristics

The apparent resistivity in pure, dry air at the operating temperature (400 °C) is shown in Fig. 4. The undoped SnO_2–TiO_2 mixtures exhibited a higher resistivity than the Sb-doped oxides. For both substituted materials the resistivity rose by two orders of magnitude upon addition of 10% mole fraction of TiO_2; then further TiO_2 substitution increased the resistivity up to $x=0.75$ with a plateau observed between $0.1<x<0.5$ for the doped materials. The specific resistivities of several sintered bodies of doped and dopant free materials were measured in the process of heating from room temperature (RT) to 700 °C and back to RT. The materials prepared by the homogenisation method (spinodally decomposed materials) and sintered at 1000 °C exhibited a lower resistivity than those prepared by ball-milling whereas the ones sintered at 1200 °C exhibited similar behaviour to the single phase materials. The activation energies (E_A) for electric conduction as a function of composition, x, were calculated from the slope of the $(\ln R-1/T)$ temperature variation, in the range 400–550 °C, and are shown in Fig. 5.

The $Ti_x(Sn_ySb_{1-y})_{1-x}O_2$ pellets all showed a decrease in resistance upon exposure to ppm concentrations of reducing gases CH_4, C_3H_8 and CO as well as H_2O, which classifies these materials as n-type semiconductors. The sensitivity, defined as the ratio $\Delta\sigma/\sigma_0=(R_{air}-R_{gas})/R_{gas}$, where σ denotes conductivity (σ_0 in pure air) of the compounds to 1% methane and carbon monoxide in dry air at different temperatures (400, 500 and 600 °C) as a function of composition is given in Fig. 6.

The sensitivity of the single phase $Ti_x(Sn_{0.99}Sb_{0.01})_{1-x}O_2$ decreased across the series from $x=0.1$ to $x=0.75$ upon exposure to CH_4 and to $x=0.5$ upon exposure to CO, and subsequently increased from this x value to pure TiO_2. This pattern of behaviour was maintained for all the operating temperatures studied. Overall the sensitivity of all the materials followed $S_{C_3H_8}>S_{CO}>S_{CH_4}$. The conventional interpretation ascribes such differences in sensitivity to different gases to differences in the rate constant for reaction of the gas with the electrically active surface states;[4] such variations are also

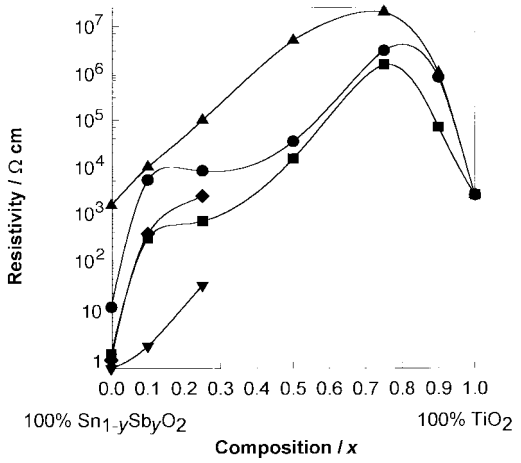

Fig. 4 Resistivity *vs.* composition (x) at 400 °C for $Ti_x(Sn_{1-y}Sb_y)_{1-x}O_2$: (●) 1%Sb; (■) 5%Sb, ball milled; (▲) dopant free; (▼) 5%Sb (homogeniser fired at 1000 °C); (◆) 5%Sb (homogeniser fired at 1200 °C).

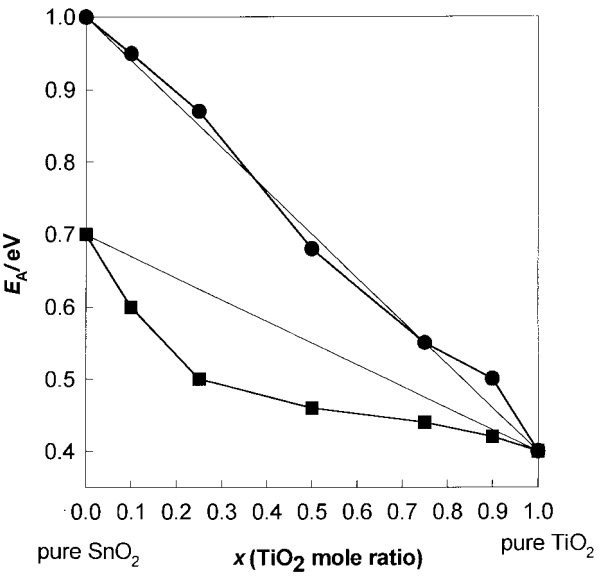

Fig. 5 Activation energy for conduction in the temperature range 400–550 °C *vs.* composition for the solid solution materials. (●) 0% Sb; (■) 1% Sb.

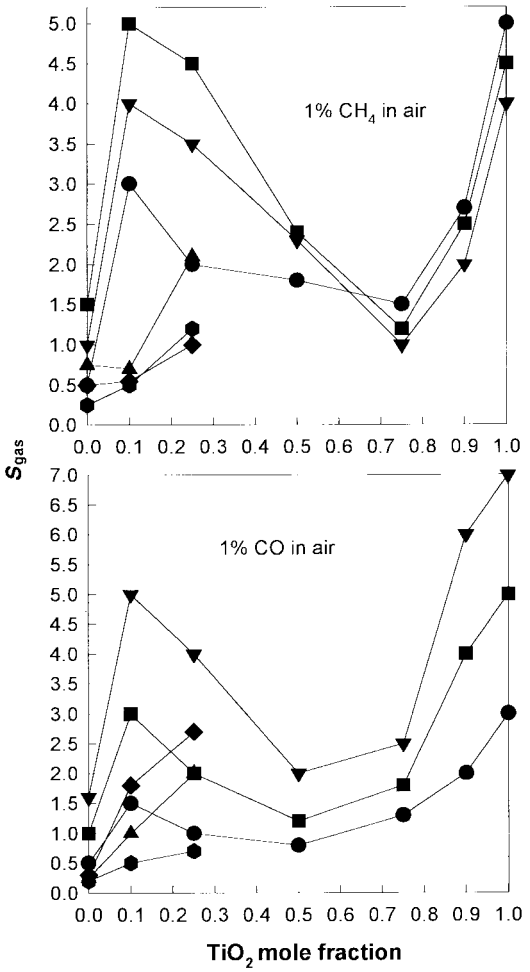

Fig. 6 Sensitivity *vs.* composition for $Ti_x(Sn_{0.99}Sb_{0.01})_{1-x}O_2$ to CO and CH_4, determined at different operating temperatures for materials prepared at different firing temperatures. Materials fired at 1200 °C in the composition range of spinodal decomposition showed results intermediate between those shown by the solid solution materials (fired at 1400 °C) and those fired at 1000 °C. Solid solutions: (▼) 400 °C, (■) 500 °C, (●) 600 °C; spinodally decomposed: (◆) 400 °C, (▲) 500 °C, (◆) 600 °C. Sensitivity, $S=\Delta\sigma/\sigma_0=(R_0-R)/R$ where R denotes resistance and σ conductivity (R_0, σ_0 in pure air).

sensitive to the temperature and the geometry of the gas-sensitive layer.[20] Typically, for the present preparations, $S_{C_3H_8}/S_{CO}\sim1.5$. The 1% doped materials were overall more sensitive to CO and CH_4 than the 5% doped ones. A plot of sensitivity to water (S_{H_2O} at 100% RH, 20 °C) *vs.* composition is given in Fig. 7. A maximum in sensitivity was observed at 10% TiO_2 mole ratio. This maximum was at the same composition as the maximum in sensitivity to other gases, but the behaviour on further increase of Ti content was clearly different to that observed for other gases, there being no minimum followed by a second maximum.

The spinodally decomposed materials ($0<x<0.25$) showed sensitivity to all gases similar to that of single-phase materials. Nevertheless, whereas the sensitivity of single-phase materials rose upon introduction of 10% mol fraction of TiO_2 and subsequently decreased at higher composition, the sensitivity of the spinodally decomposed materials increased monotonically with composition over the range studied.

Discussion

Behaviour of single-phase materials

Variation of baseline in air with composition of the material. The variation of both conductance (Fig. 4) and conductance

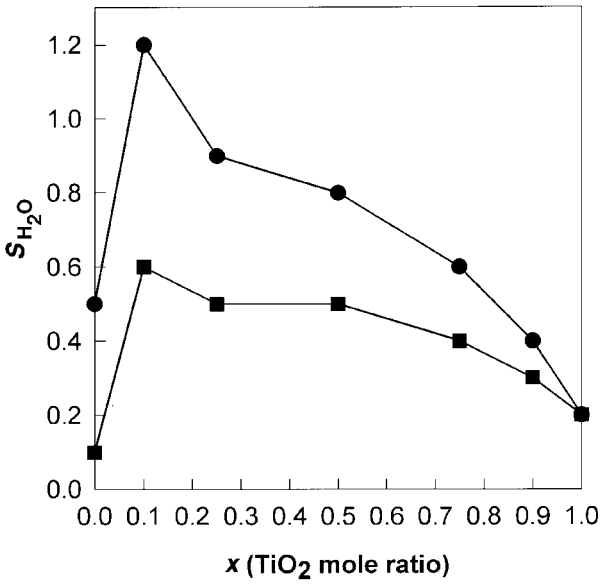

Fig. 7 Sensitivity to water, $(R_{dry}-R_{wet})/R_{wet}$ *vs.* composition at 415 °C for $Ti_x(Sn_{1-y}Sb_y)_{1-x}O_2$ solid solutions. R_{dry} denotes the resistance in pure, dried air and R_{wet} that in pure air saturated with water vapour at room temperature (≈20 °C); $y=0.01$ (●), 0.05 (■).

activation energy (Fig. 5) with composition taken together with the variation of surface composition (Fig. 3) show that there is some subtle interplay of different effects which it is necessary to interpret before interpreting the gas behaviour. The behaviour of pure SnO_2 has been interpreted as that of an extrinsic semiconductor in which the trap states controlling the conductivity are oxygen species at the surface of the crystallites.[1,4,19] The model, at the two extremes, is either a surface trap limited conductance[19] or a Schottky barrier controlled conductance.[4] The activation energy for conduction is then either the energy gap between surface state and conduction band edge (ΔE_S) or the surface barrier height whilst the charge carrier concentration is controlled by the concentration of bulk donor states. Given that the band gap of SnO_2 and TiO_2 are respectively 3.6[23] and 3.0 eV[24] and that the bulk donor states Sn''_{Sn} and Ti'_{Ti} are respectively ≈0.15 and 0.8 eV below the conduction band edge in the pure oxides SnO_2 and TiO_2 (110),[25] this interpretation is reasonable as discussed below.

So, for the undoped materials, the activation energy for conduction decreases linearly with increase of TiO_2 mole fraction (Fig. 5), from 1 eV for pure SnO_2 to 0.4 eV for pure TiO_2. This is consistent with a surface trap limited conductivity with the position of the surface trap level with respect to the valence band edge (oxygen p-states) remaining approximately constant with change of composition. Hence, as the band gap decreases from SnO_2 to TiO_2, ΔE_S decreases also. The interpretation of measurements of activation energy deduced from variation of conductance over a limited temperature range is fraught with difficulty, however, especially for porous pellets where charge carrier activation from surface states as well as from bulk donors and across the band gap all contribute to the measured conductivity. Our measured activation energy for porous SnO_2 is too low for band-gap excitation and too high for excitation from bulk donors, but consistent with other measurements which have been interpreted as surface trap- or Schottky barrier-limited conductance determined by the surface trap state energy.[1,4] The activation energy for conduction of TiO_2 reported here is significantly lower than that reported elsewhere, including our own measurements on Nb-doped TiO_2 porous pellets (≈1 eV,[26] an intermediate value consistent with a transition range between conduction dominated by activation from bulk defects and conduction activated

across the band gap). We assume that the present measurements gave a lower value because they were dominated by activation from the surface state, and that this was observed because the pellets were highly porous and the material was undoped, so that there was no defect compensation effect.[27]

The effect of Sb addition was markedly to decrease the activation energy for $(Sn–Sb)O_2$. The interpretation is straightforward: increase of Sb concentration increases the donor concentration which decreases both the Debye length (so that a surface trap-limited model becomes inappropriate) and the surface barrier height. In this case, the conduction activation energy is taken to be the surface barrier height.

For the undoped materials, the decrease in conductivity with addition of TiO_2 to SnO_2 implies a decrease in bulk donor density; to a minimum when $x_{TiO_2} \approx 0.8$. Trace impurities in the oxides (*e.g.* trivalent elements such as Fe and Al), at different concentration in the two oxides, might cause this effect. More spectacular is the effect of addition of TiO_2 to the Sb-doped SnO_2, where the addition of a small amount of Ti caused a decrease in conductivity by two to three orders of magnitude. Since the Sb/Sn ratio is maintained constant, addition of Ti would dilute the Sb and hence decrease the charge carrier concentration. The effect is not, however, linear in TiO_2 mole fraction. It seems that Ti substitution enhances the surface segregation of Sb and thus decreases the bulk donor density more than expected by the simple effect of dilution. The surface might even be saturated in Sb. The sharp decrease in activation energy also caused by Ti substitution into the doped material might be interpreted as an effect of the surface segregation upon the surface barrier height, perhaps because there would be consequentially a non-uniform spatial distribution of bulk donor states. For the Sb-doped materials, therefore, for compositions where $(Sn–Sb)O_2$ is the major constituent, the behaviour should be dominated by the distribution of Sb between bulk and surface. This effect would explain the plateau in conductivity for $x_{TiO_2} = 0.1$–0.5. When TiO_2 becomes the major constituent, the behaviour of the undoped and doped materials becomes similar.

The small shifts in core level binding energy (Table 2), seem correlated with the changes in electrical behaviour. The Ti $2p_{3/2}$ binding energy goes through a maximum when the resistivity is maximum. The Sn $3d_{5/2}$, Sb $3d_{3/2}$ binding energies have a minimum corresponding to the plateau in resistivity. These binding energy shifts probably reflect changes in the metal environment, since changes in Fermi level would cause the same direction of shift for all the cations. The gas response of these compounds was mediated at a surface with a quite different composition to the bulk (Fig. 3). Thus, the effects of dopant density and surface composition are intimately linked. Hence, the cation composition of the lattice had an effect on the dopant density by changing the electron occupancy of non-bonding states localised on the metal, and altering the dopant density by changing the Sb concentration changed the surface composition as a result of surface segregation.

Variation of gas sensitivity with composition. The effect of surface acceptor-state density on the conductivity of n-type porous metal oxides in the limit of low bulk-donor density (surface-trap limited model) has been formulated previously.[19] The conductivity can be expressed in terms of surface acceptor-state density,

$$\sigma/e = \mu_e K_1 (N_A + N_D)/N_S + \mu_p K_2 N_S/(N_A + N_D) \qquad (1)$$

Here, equilibrium between surface acceptors (oxygen species) with the conduction and the valence bands can be expressed as:

$$S^- \rightleftharpoons S + n';$$

$$K_1 = N_c \exp(-\Delta E_S/kT)$$

and

$$S \rightleftharpoons S^- + p^{\cdot}$$

$$K_2 = N_V \exp[-(\Delta E_G - \Delta E_S)/kT]$$

where N_A and N_D denote the bulk concentrations of acceptor and donor states, respectively. Here, also, N_V and N_C are the densities of states at the valence and conduction band edge, ΔE_G represents the band gap, ΔE_S is the surface state energy with respect to the conduction band edge and N_S denotes the total surface state density. If the majority of charge carriers are electrons then the first term of equation (1) dominates, and if holes then the second.

The dependence of the conductivity on the surface trap concentration, *i.e.* the sensitivity, S, to the presence of a reactive gas in the air, is obtained in a form which can be compared with experimental data by differentiating eqn. (1) with respect to N_S.

$$S = \frac{d(\sigma/e)}{dN_S}\left(\frac{1}{\sigma_0/e}\right) = \frac{1}{N_S}\left(\frac{[\mu_p K_2 N_S/(N_A+N_D)] - [\mu_e K_1 (N_A+N_D)/N_S]}{[\mu_p K_2 N_{S,0}/(N_A+N_D)] + [\mu_e K_1 (N_A+N_D)/N_{S,0}]}\right) \qquad (2)$$

If the change in surface trap state concentration is not too large, so $N_S \approx N_{S,0}$, then

$$S \approx \frac{1}{N_S}\left(\frac{1-\alpha}{1+\alpha}\right) \qquad (3)$$

with

$$\alpha = \frac{\mu_e K_1 (N_A + N_D)^2}{\mu_p K_2 N_S^2}$$

The effect of a reactive gas is interpreted as a decrease of N_S. With $\alpha < 1$, the conductivity decreases with decrease of N_S: this is a 'p'-type response. With $\alpha > 1$, conductivity increases with decrease of N_S: this is an 'n'-type response. For n-type semiconducting oxides such as $Ti(SnSb)O_2$, the sensitivity according to this compensated surface-trap limited model will show a strong dependence on N_S. The magnitude of K_1 and K_2 is controlled by the surface acceptor-state energy, ΔE_S. Hence, since the value of K_1/K_2 varies exponentially with ΔE_S, small changes in the surface acceptor-state energy could have a large effect on the sensitivity.

Eqn. (3) explains the broad features of the variation in response to methane and carbon monoxide with variation of composition, in the range $x_{TiO_2} = 0.1$–1. Taking the undoped materials first, Fig. 4 was interpreted as showing a decrease in N_D with composition, in the range $x_{TiO_2} = 0$–0.8, followed by an increase in N_D with further increase in x_{TiO_2}. Fig. 5 was interpreted as showing a linear decrease of ΔE_S with increase of x_{TiO_2} over the whole range. A linear decrease of ΔE_S with increase of x_{TiO_2} would cause an exponential increase in K_1/K_2. Fig. 6 shows a steady decrease in sensitivity to CO and CH_4 with increase of x_{TiO_2} in the range 0.1–0.8; with a minimum at $x_{TiO_2} = 0.8$ and then an increase with further increase of x_{TiO_2}. In this, the variation of sensitivity exactly parallels the variation of conductivity and the variation of N_D. According to eqn. (3), in the range $x_{TiO_2} = 0.1$–0.8, the decrease in N_D would act to decrease the sensitivity whereas the increase in K_1/K_2 would act to increase it. Over the range $x_{TiO_2} = 0.8$–1, we presume that the increase in sensitivity is due both to the increase of K_1/K_2 and the increase of N_D. Qualitatively, therefore the variation in sensitivity is explained.

What is not explained by eqn. (2) is the marked increase in sensitivity from $x_{TiO_2} = 0$ to $x_{TiO_2} = 0.1$. Furthermore, Sb doping of SnO_2 increases N_D but markedly decreases sensitivity. Both facts draw attention to the assumption of a surface trap-limited conductivity in fully depleted crystallites, which underlies eqn. (2). The behaviour can be interpreted both by

a Schottky barrier-limited conductivity model and by the effects of doping upon barrier height and Debye length. Increasing donor density decreases surface barrier height and Debye length. Both effects give a decrease in sensitivity. Decreasing donor density would then increase sensitivity. Fig. 3 and 4 have been interpreted by a marked decrease in donor density caused by Ti addition to the doped materials. Therefore, the increase in sensitivity in the range $x_{TiO_2}=0$–0.1 is interpreted as the effect of decreasing donor density causing an increase in Debye length and leading to a transition from a surface barrier-limited to a surface trap-limited regime.

Comparison of sensitivity to water vapour with that to other gases. The notable difference between the effects of water vapour and those of CO and CH_4 is that the increase in sensitivity for $x_{TiO_2}=0.8$–1 was not observed. Eqn. (3) gives a framework for interpretation. The increase in sensitivity to CH_4 and CO was interpreted above as an effect of variation of N_D dominating an effect of variation of K_1/K_2. However, if the binding site for water were different to the reaction site for other gases, that is if K_1 were different, then the result might be different. It has been shown before[22,28] that an assumption of a different value of K_1 for states associated with water, K_{1,H_2O}, would be plausible. It was further shown that an assumption of K_{1,H_2O} which was sensitive to the surface composition would also be plausible. Therefore, the monotonic decrease of S_{H_2O} with x_{TiO_2} is interpreted, within the framework of eqn. (2), as the result of a monotonic decrease in K_{1,H_2O} which dominates over the effect of increasing N_D for $x_{TiO_2}>0.8$.

Behaviour of materials decomposed by spinodal mechanism

One objective of the present work was to assess whether there was a special effect associated with the spinodal decomposition. Such effects could be caused for example by the segregation of the dopants to the spinodal boundaries resulting in the trapping of conduction electrons on these species. From Fig. 4 the resistivity of the 5%Sb-doped material fired at 1000 °C indeed exhibited a significant difference from the single phase material which cannot be interpreted as a variation of particle size. The gas sensitivity of material fired at both 1000 and 1200 °C also showed a somewhat different variation with composition to that of the single phase material.

However, whilst it is not certain that particular effects are absent, the results can be interpreted in terms of the phase diagram[8] if it is assumed that the resistivity and gas sensitivity are determined simply by the volume fraction of the two different phases. Thus, at low x_{TiO_2}, the dominant phase is SnO_2 containing a rather smaller fraction of TiO_2 than that added. If the diagrams of gas sensitivity and resistivity are plotted in terms of mole fraction of TiO_2 in solution in SnO_2, then the behaviour of the spinodally decomposed material seems, within experimental error and taking into account possible problems due to only partial reaction, indistinguishable from that of the single phase material. Hence, within the limitation of the present work, there do not seem to be any special effects of the spinodal decomposition.

Conclusion

The variation of both conductance and conductance activation energy with composition for the single phase materials has been explained using a model which is either a surface trap limited conductance for undoped materials or a Schottky barrier controlled conductance for Sb-doped materials. The effect of dopant density and surface composition on the gas response has been explained using a compensated semiconductor conduction model. The different sensitivity to water vapour compared to other gases, especially in the range $0.8<x<1$, has been interpreted by consideration of the position with respect to the conduction band edge of states associated with water and of states associated with adsorbed oxygen. The observed behaviour implies a different variation with composition of the energies associated with these different states. The states associated with adsorbed oxygen which are responsible for the gas sensitivity lie closer to the conduction band edge in TiO_2 than in SnO_2. The surface oxygen states and surface water states lie closer together in energy in TiO_2 than in SnO_2.

Acknowledgements

This work was supported by the UK Engineering and Physical Sciences Research Council, Capteur Sensors & Analysers Ltd and the Ford Motor Company. We acknowledge the assistance of Dr K. F. E. Pratt, Dr G. S. Henshaw and Mrs Y. Wang.

References

1 J. F. McAleer, P. T. Moseley, J. O. W. Norris, D. E. Williams and B. C. Tofield, *J. Chem. Soc., Faraday Trans. 1*, 1988, **84**, 441.
2 W.-Y. Chung and D.-D. Lee, *Sens. Actuators B*, 1993, **13–14**, 517.
3 W.-Y. Chung, D.-D. Lee and B.-K. Sohn, *Thin Solid Films*, 1992, **221**, 304.
4 D. E. Williams, in *Solid State Gas Sensors*, ed. P. T. Moseley and B. C. Tofield, Adam Hilger, Bristol, 1987.
5 T. Seiyama, N. Yamazoe and H. Arai, *Sens. Actuators*, 1983, **4**, 85.
6 Y. Shimizu, H. Arai and T. Seiyama, *Sens. Actuators*, 1985, **7**, 11.
7 D. Garcia and D. Speidel, *J. Am. Ceram. Soc*., 1972, **556**, 322.
8 M. Park, T. E. Mitchell and A. H. Heuer, *J. Am. Ceram. Soc*., 1975, **58**, 43.
9 C. A. Vincent and D. C. G. Weston, *J. Electrochem. Soc*., 1972, **119**, 515.
10 P. E. Sinclair, G. Sankar, C. R. A. Catlow, J. M. Thomas and T. Mashmeyer, *J. Phys. Chem.*, 1997, **101**, 4232.
11 V. E. Henrich and P. A. Cox, *The Surface Science of Metal Oxides*, Cambridge University Press, Cambridge, 1994.
12 N. N. Padurow, *Naturwissenschaften*, 1956, **43**, 395.
13 J. W. Cahn, *Acta Metall*., 1961, **9**, 795.
14 A. H. Schultz and V. S. Stubican, *Philos. Mag*., 1968, **18**, 929.
15 P. K. Gupta and A. R. Cooper, *Philos. Mag*., 1970, **21**, 611.
16 J. Takahashi, M. Kuwayama, H. Kamiya, M. Takatsu, T. Oota and I. Yamai, *J. Mater. Sci*., 1988, **23**, 337.
17 T. C. Yuan and A. V. Virkar, *J. Am. Ceram. Soc*., 1986, **69**, C310.
18 T. C. Yuan and A. V. Virkar, *J. Am. Ceram. Soc*., 1988, **71**, 12.
19 D. E. Williams and P. T. Moseley, *J. Mater. Chem.*, 1991, **1**, 809.
20 G. S. Henshaw, L. J. Gellman and D. E. Williams, *J. Mater. Chem.*, 1994, **4**, 1427.
21 C. D. Wagner, in *Practical Surface Analysis*, 2nd edn., vol. 1 *Auger and X-ray Photelectron Spectroscopy*, ed. D. Briggs and M. P. Seah, Wiley, Chichester, 1990, p. 595.
22 V. Dusastre and D. E. Williams, *J. Phys. Chem. B*, 1998, **102**, 6732.
23 D. C. Cronemeyer, *Phys. Rev.*, 1952, **87**, 876.
24 K. J. Button, D. G. Fonstad and W. Drey-Bradt, *Phys. Rev. B*, 1971, **4**, 4539.
25 I. Manassidis, J. Goniakowski, L. N. Kantorovich and M. J. Gillan, *Surf. Sci.*, 1995, **339**, 258.
26 G. S. Henshaw, L. Morris, L. J. Gellman and D. E. Williams, *J. Mater. Chem.*, 1996, **6**, 1883.
27 N. G. Eror, *J. Solid State Chem.*, 1981, **38**, 281.
28 G. S. Henshaw, V. Dusastre and D. E. Williams, *J. Mater. Chem.*, 1996, **6**, 1351.

Paper 8/07380E